

Chapter 1

Introduction

The aim of prestack seismic imaging is to obtain an estimate of the reflectivity of the subsurface from a seismic survey conducted on the surface. A basic requirement for this process is the ability to propagate a seismic wavefield through the subsurface. In order to propagate the wavefield we need to know the subsurface velocity structure. This appears to create an impasse, we need to know the subsurface structure in order to image the subsurface structure. Fortunately this problem is not insurmountable, the imaging and the velocity estimation can be performed as a coupled process. As the estimate of the velocity structure improves, the image improves, and vice versa.

A well known testbed for the issues involved in prestack imaging and velocity estimation is the “Marmousi” dataset. The dataset was originally created by the Institut Français du Pétrole as a test of velocity inversion methods. It was distributed as a “blind test” dataset. The participants in the trial were given a synthetic seismic dataset and two well logs. They then attempted to invert the data to obtain a velocity model. The results of this blind test are described in Versteeg and Grau (?).

After the blind test was complete, the true velocity model was published. The dataset has since become a very popular testbed for pre-stack imaging algorithms. At this point a horrible discovery was made, some imaging methods could not produce a good image of the structure in the model even when they were given a *perfect* velocity model. In particular several authors have noted the poor results obtained with prestack Kirchhoff migration algorithms.

The aim of this introduction is to describe why Kirchhoff migration algorithms are popular, why they fail, and suggest a strategy that can be used to remedy the deficiencies in the current implementations.

There are two main classes of imaging algorithms.

1. Algorithms that use recursive wavefield continuation to backwards propagate the received wavefield in space or time.
2. Non-recursive algorithms that formulate the imaging processes as an integral equation involving the Green’s functions of the wave equation.

The integral methods are the most popular methods for prestack imaging, because the recursive methods often require a regular spatial sampling and can be very expensive.

A generic integral form for a prestack imaging algorithm is,

$$\text{Image}(\mathbf{x}) = \int \int_S \int_R W(\mathbf{x}_S, \mathbf{x}_R, \mathbf{x}, \omega) G^\dagger(\mathbf{x}_S, \mathbf{x}, \omega) G^\dagger(\mathbf{x}, \mathbf{x}_R, \omega) \text{Data}(\mathbf{x}_S, \mathbf{x}_R, \omega) d\mathbf{x}_S d\mathbf{x}_R d\omega.$$

$G^\dagger(\mathbf{x}_1, \mathbf{x}_2, \omega)$ is the adjoint of the Green’s function from point x_1 to x_2 . $\text{Data}(\mathbf{x}_S, \mathbf{x}_R, \omega)$ is the measured wavefield for a particular source-receiver pair. In this equation, W is a weight function that is algorithm dependent. For a simple migration algorithm that is only designed to generate a structural image this weight might be one. For a migration/inversion algorithm that attempts to recover the true reflectivity as well as the structure, the weight will be a function of frequency, source location, receiver location, and image coordinates.

In seismic data processing, algorithms of this form are often called “Kirchhoff Migration” algorithms. Indeed, integrals of this form can be derived from the Kirchhoff integral. There are also many other paths that can be used to derive an integral of this form, but the resulting algorithms are still referred to as “Kirchhoff migration” or “Kirchhoff imaging”. I will use the phrase to refer to any algorithm of this form whether or not it is derived from the Kirchhoff integral.

This algorithm requires the estimation of the Green’s function for every surface (source or receiver) location and every frequency. This may be prohibitively expensive and require unreasonable amounts of storage. A common simplification is to parameterize the Green’s function by one or more events in the time domain. Each event is defined by a traveltimes, an amplitude, and a phase. Most methods for calculating these parameters use a high frequency approximation to the wave equation. In this thesis I present a method that calculates these parameters without making a high-frequency approximation. I call this method “band-limited Green’s function estimation.”

1.1 Full Green’s functions

If the medium has properties that are a function of both horizontal and vertical coordinates a wide-band Green’s function should be calculated for every surface location. Using currently available computers, it is too expensive to routinely calculate these functions for all frequencies. Given current progress in computer technology, this could change rapidly. In the near future it may be practical to calculate all the Green’s functions for a 2-D survey. However, a huge increase in computer power will be required to calculate them all for a 3-D survey.

Apart from the cost of calculating the Green’s functions the other consideration is the space required to store them. If the complete Green’s function is stored that space is very large. The Green’s function has one extra dimension, depth, that the surface seismic data does not have. A 2-D prestack seismic dataset is a 3-D volume it has axes of shot location, receiver location, and time or frequency. A full Green’s

function for a 2-D dataset is a 4-D volume with axes of surface location, subsurface location, depth, and time or frequency. A 3-D prestack dataset is a 5-D volume with two shot coordinates, two receiver coordinates and time or frequency. A full Greens' function for a 3-D survey is a 6-D volume.

Table 1.1 shows some typical data volumes for the 2-D and 3-D prestack data. For each survey I have estimated the numbers of stacked inline and crossline output locations and the average stack-fold at each location. This gives an estimate of the number of traces recorded in the field. Given the number of traces and an estimate of the number of time samples, I can calculate the size of the complete dataset.

Data Type	Inline	X-line	Fold	Time	Storage
2-D prestack	1000	1	100	1500	600MB
3-D prestack marine	1000	1000	100	1500	600GB
3-D prestack land	300	200	50	1000	12GB

Table 1.1: Seismic Data volumes for 2D and 3D prestack data.

Table 1.2 shows the storage required for the full broadband Green's functions for these surveys. The cost of calculating the Green's functions, and the cost of the imaging algorithm are both approximately proportional to the size of the storage required for them. Thus, this table can also be used as a rough estimate of computational cost. In this table I use the same number of surface locations but for each location I assume that an aperture of $\pm 2000\text{m}$ is required in the marine survey and 1000m in the land survey. When sampled at a 25m spacing this creates 160 offsets for the marine case and 80 for the land case. These numbers are ridiculously large, there is no good way

Data Type	Inline	X-line	X-offset	Y-offset	Frequency	Depth	Storage
2-D prestack	1000	1	160	1	250	400	122GB
3-D prestack marine	1000	1000	160	160	250	400	18626TB
3-D prestack land	300	200	80	10	150	250	14TB

Table 1.2: Storage for the full Green's functions for 2D and 3D datasets.

to store 18626TB in the foreseeable future. In practice the Green's functions might be calculated on a much sparser grid and interpolated on the fly as they are used. An eight fold subsampling in each surface dimension and a subsampling by a factor of two in each of the other dimensions may be reasonable. The Green's function sizes for the subsampled case are shown in Table 1.3. Even with this amount of subsampling it still requires a 36TB dataset to be stored for the 3-D marine example, fifty times as much data as was recorded in the field.

Data Type	Inline	X-line	X-offset	Y-offset	Frequency	Depth	Storage
2-D prestack	125	1	80	1	250	200	4GB
3-D prestack marine	125	125	80	80	250	200	36TB
3-D prestack land	38	25	40	5	150	125	26GB

Table 1.3: Storage for subsampled Green’s functions for 2D and 3D datasets.

1.2 Parametric Green’s functions

One common way to overcome the problems associated with using the full Green’s function is to use a parametric form of the Green’s function. The parametric form most commonly used is one that describes the Green’s function in terms of impulsive events in the time domain.

$$G(\mathbf{x}_1, \mathbf{x}_2, \omega) = A(\mathbf{x}_1, \mathbf{x}_2)e^{-i\omega\tau(\mathbf{x}_1, \mathbf{x}_2)}$$

A is the (possibly complex) amplitude of the event and τ is the travelttime.

This form has the advantage that the generic imaging algorithm in the frequency domain (1) can be transformed to the time domain, where it becomes a surface integral rather than a volume integral (see chapter ??). This produces a huge decrease in the cost of the imaging method.

The other major advantage is that we only need to store three real-valued coefficients for each Green’s function, rather than a complex number for each of several hundred frequencies. The storage requirements for the parametric form after subsampling are given in Table 1.4. Storing this amount of data online is feasible with today’s technology.

Data Type	Inline	X-line	X-offset	Y-offset	Parameters	Depth	Storage
2-D prestack	125	1	80	1	3	200	23MB
3-D prestack marine	125	125	80	80	3	200	224GB
3-D prestack land	38	25	40	5	3	125	270MB

Table 1.4: Storage for parametric Green’s functions for 2D and 3D datasets.

1.2.1 Asymptotic Green’s functions

In the high frequency limit, the unknowns in the parametric form for the Green’s function can be calculated directly. In the simplest schemes τ is found by solving the eikonal equation and A is found by solving the transport equation. A wide variety of

methods are available to solve these problems. For example, finite difference solutions to the eikonal equation (?), graph theoretic calculation of fastest paths (?), dynamic ray tracing (?), paraxial ray tracing (?).

All these methods have one thing in common, they solve a high frequency approximation to the wave equation. They are only good approximations to the solution in the seismic bandwidth if the slowness model is smooth on a scale that is long compared to the seismic wavelength. Beydoun and Ben-Menachem (?) give estimates of the regimes of validity of these schemes.

Some schemes have an additional limitation. When there are multiple arrivals present in the data, calculating all the arrivals can become complicated. Some implementations calculate only the first arriving events. In particular, finite difference solutions to the eikonal equation can calculate the first arrivals very efficiently, but they do not model the later arrivals. If the first arrival contains little energy, the solution obtained will be a poor approximation of the full Green's function.

1.2.2 Frequency dependent traveltimes

In asymptotic ray tracing the traveltime of high-frequency energy to some location is merely the line integral of the slowness along the ray to that point. This is not true for waves of finite frequency. Woodward and Rocca (?) demonstrated that the traveltime of band-limited energy is related to the volume integral of slowness over a "wavepath" between the source and receiver. In their work they calculated the wavepath by finite-difference calculation of the Green's functions. The width of the wavepath is frequency dependent, this means that seismic data in different frequency bands can have different traveltimes; the wavelet is dispersed. Figure 1.1 shows a schematic plot of a phase/frequency relationship for one location. The group slowness at any frequency is given by the slope of the curve. In the high frequency limit the curve is a straight line, all the high frequencies arrive at the same time. In contrast the low frequencies arrive at different times. If the seismic frequency band on this plot is "band2", the asymptotic solution will be a good approximation to the seismic traveltime. If the seismic frequency band is "band1", then the asymptotic solution will not be a good approximation to the seismic traveltime. However the straight line labeled "band-limited traveltime" is a good approximation to the curve within band2. The aim of my method is to estimate this traveltime rather than the traveltime given by the asymptotic solution.

Several authors have attempted to account for the band-limited nature of seismic energy while remaining within the framework of a ray tracing scheme. Biondi (?) uses an approximation to the Helmholtz equation to calculate a frequency-dependent "effective-slowness field" through which conventional ray tracing can be performed. Červený and Soares (?) propose integrating slowness in a "Fresnel-volume" around the central ray path. Schuster and Quintus-Bosz (?) calculate tomographic back projections that use traveltimes from the eikonal equation but attempt to account for the band-limited nature of the seismic data. Others have used less formal schemes

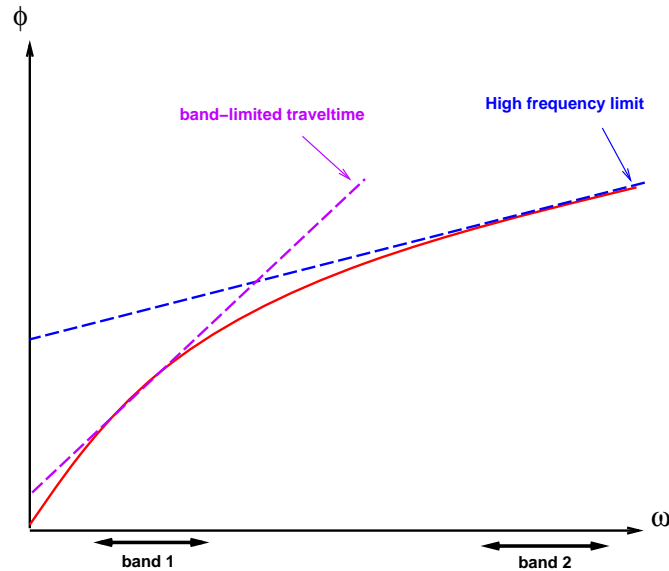


Figure 1.1: Phase as a function of frequency for a simple dispersed event. (Intro-phasecurve) [NR]

with a similar flavor. Lomax (?) performs ray tracing in a slowness field that is smoothed ahead of each ray. Michelena and Harris (?) use finite-width “natural-pixels” to invert traveltimes of seismic data in cross-well tomography. The natural-pixels are a constant-width approximation to the true wavepath.

1.2.3 Band-limited Green’s functions

In this thesis I present a method that uses the parametric representation of the Green’s function, so that storage costs and the cost of imaging the data are the same as for asymptotic methods. However in my scheme the Green’s functions are calculated in the same frequency band as the seismic data. The cost of calculating the Green’s function is greater than simple asymptotic methods but much less than full wave equation methods.

In chapter ??, I examine some methods for obtaining mono-frequency Green’s functions. The complete Green’s function is the superposition of all such mono-frequency Green’s functions. The cost of calculating the Green’s function for a single frequency is similar to the cost of a finite difference scheme to solve the eikonal equation. For a medium that has properties that depend only on depth only one set of Green’s functions needs to be calculated. The same Green’s function is used for all surface locations. In chapter ??, I demonstrate prestack modeling and migration algorithms using a single set of Green’s functions.

In chapter ??, I demonstrate that the parametric form of the Green’s function can be estimated from a few mono-frequency Green’s functions calculated at selected frequencies. These traveltimes and amplitudes are calculated in the seismic frequency

band not at high frequency. The traveltimes and amplitudes that my particular implementation calculates are those of the maximum energy arrival. If only one event is to be chosen it is much better to use the maximum energy event rather than the first arriving event. It is the best single event approximation to the full Green's function (in the L_2 norm).

In chapters ?? and ??, I use this method to calculate band-limited Green's function in the Marmousi model. These Green's functions are then used to image the Marmousi dataset. The use of band-limited Green's function gives results that are similar to those from more expensive algorithms that use recursive extrapolation of the wave equation. Figure 1.2 shows a close up of four images of the reservoir in the Marmousi model that were created by migrating the Marmousi dataset. The first

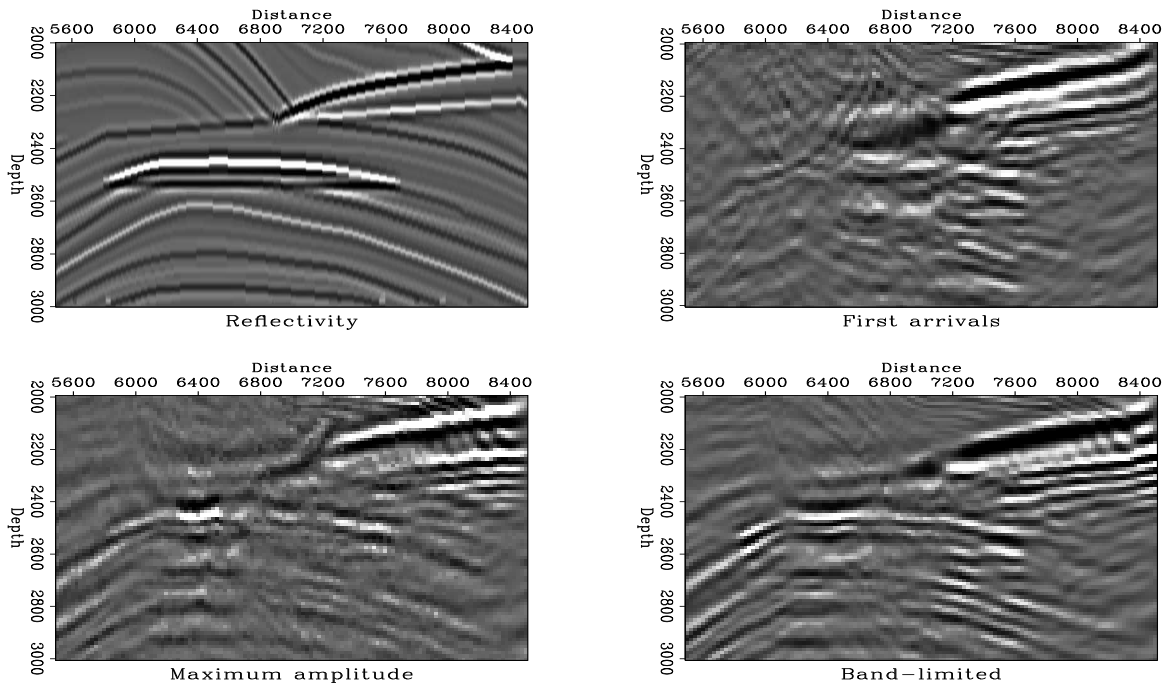


Figure 1.2: Comparison of migrations using three travel time estimation methods. left: ideal result, top right frame: first arrival traveltimes, bottom left: maximum amplitude traveltimes from ray tracing, bottom right: maximum energy band-limited traveltimes. [Intro-migex](#) [NR]

image shows the ideal result. The second shows the result created using first arrival travel times. The third image was created using maximum amplitude traveltimes calculated by paraxial ray tracing. The fourth image was created using maximum energy traveltimes calculated using my method. I contend that my method has produced the image that is closest to the ideal result.

1.2.4 Relationship with other methods

Figure ?? shows the intended relationship of my algorithm to other Green's function estimation methods. The horizontal axis is the "normalized wavenumber" of the seis-

mic wavefield. The wavenumber of the seismic data is normalized by the wavenumber of the model variation. If the data has a high normalized wavenumber the medium is ray valid. In that situation a ray tracing method or other eikonal equation solution method is the best way to calculate the Green's function. If the wavelength of the model variation is of the same order as the wavelength of the seismic data, or if there are many discontinuities in the model then a ray-based method may not be suitable. This region is the one that I have labeled "seismic bandwidth" on the horizontal axis of the figure.

The ideal algorithm "Perfection" would calculate a good approximation to the full Green's function in the seismic frequency band at very low cost. A finite difference solution of the eikonal equation is very cheap but it gives a poor solution when the medium is not smooth. At the other extreme are finite difference solutions to the two-way and one-way wave equations. They give a good solution in the seismic frequency band but they are much more expensive to calculate and more expensive to use in imaging. My method is intended to fall somewhere in between these extremes. It costs much less than full Green's functions, or reverse time migration, and only about two to eight times as much as a finite difference solution to the eikonal equation. Its virtue is that it gives a parametric approximation to the Green's function that is valid in the seismic frequency band.

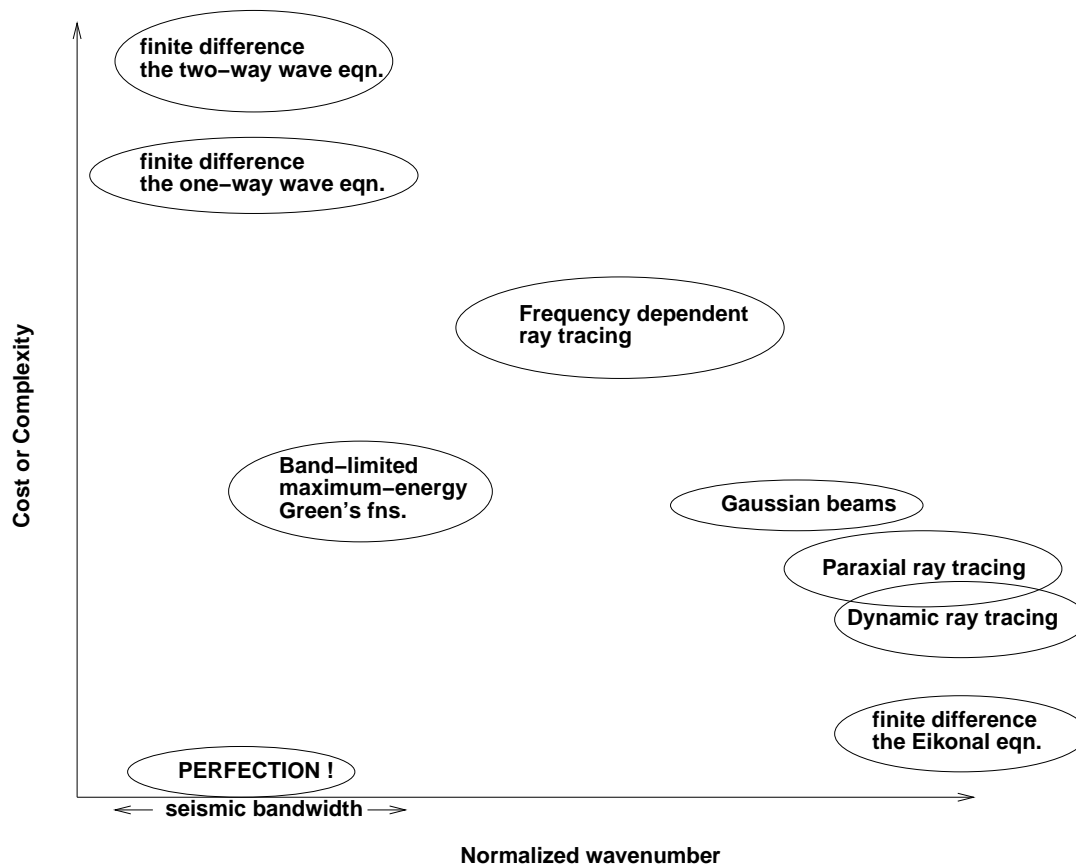


Figure 1.3: Frequency range of validity of various algorithms plotted against the cost or complexity of implementation. Not to scale. (Intro-algorithms) [NR]